Int. J. Pres. Ves. & Piping **57** (1994) 21–29

Rupture of pressurised tubes by multiple cracking and fragmentation

I. J. Ford

Theoretical Studies Department, AEA Industrial Technology, Building 424.4, Harwell Laboratory, Didcot, Oxfordshire, UK, OX11 0RA

(Received 6 August 1992; accepted 20 September 1992)

The likelihood of stable propagation of an axial crack away from a rupture site in a pressurised tube is a problem of concern in a number of areas, including the gas and nuclear industries. A model of crack propagation is developed which provides the crack velocity and deformation geometry and predicts a minimum driving pressure. Emphasis is placed upon the stability of propagation against small perturbations. The model also offers a criterion for the appearance of multiple cracks and subsequent fragmentation of the tube wall due to excessive bending strains. Calculations of interest in gas pipeline rupture and fast reactor fuel pin failure are presented.

1 INTRODUCTION

As part of constructing a safety case for a fast reactor, sequences of events are considered which lead to the rupture of the fuel pins by a build up of internal pressure, largely due to the melting of the fuel contained within the cladding tube. The subsequent ejection of fuel into the coolant channels, and the later development of the accident are then determined by the mode of failure. The cross-sectional area of the hole produced in the cladding will determine the rate of fuel ejection, and the axial extent of the opening will have an important bearing on subsequent axial fuel motion.

Although a rupture which remains axially localised presents the possibility of fuel concentration at the failure site, the opposite extreme, where a rip propagates large distances, 'unzipping' the fuel pin, could lead to the coherent release of a large proportion of the fuel into the channels. Experimentally, most pin failures have produced ruptures which extend only short distances axially[1] although at least one test has resulted in the propagation of a crack exposing half the fuel column. Clearly, it would be an advantage to be able to predict the extent of rupture propagation in a variety of conditions.

A model of the process has been developed,[2] based on mechanistic considerations of the energetics of a running crack in a cylindrical tube, and on simple ideas concerning the depressurisation of the pin, which ultimately arrests the crack. The model treats a single axial crack in the cladding, running in opposite directions away from the failure site, leaving the clad cross-section deformed into a U-shape. The parameters of the model were not completely determined in Ref. 2, however, and the deformation was arbitrarily chosen to be maximal for the single crack geometry. That is, the peak strain in the deformed cladding was taken to be equal to the remaining ductility of the clad. This is not a requirement, however, but rather a criterion for the appearance of multiple cracks and the rapid fragmentation of the cladding. It is the aim of this paper to determine the clad deformation by a consideration of the mechanics of the crack, and therefore to obtain a proper description of conditions which lead to multiple cracking and fragmentation. Clearly, the break-up of the clad will expose a greater area of fuel and lead to a more rapid ejection of material. A second consideration is that multiple cracking may lead to the early arrest of the crack.

Section 2 considers the mechanics and geometry of a crack in steady state motion, leading to a partial determination of the clad deformation and an equation for the crack velocity. Section 3 describes experimental results on crack propagation in highly pressurised gas pipelines and considers a model of gas decompression. The data are used to fix a remaining parameter of the model. Finally, in Section 4 the propagation of axial cracks in fuel pin cladding tubes is considered, leading to the application of the clad fragmentation criterion. Some comparisons with experiments from the CABRI-1 programme[1] are made and the mechanism of pin depressurisation is considered. The model is discussed in Section 5 and conclusions are given in Section 6.

2 CRACK MECHANICS AND GEOMETRY

A revised description of crack geometry has been adopted, based on the deformation observed in a series of tube rupture experiments.[3] Cross-sections of the tubes were deformed into broken circles, as illustrated in Fig. 1. Previously[2] the radial displacement of the tube wall was assumed to have a quadratic dependence on azimuthal angle, measured from the point opposite the fracture. The radial displacement $w(z, \theta)$ is now taken to be

$$w(z, \theta) = \begin{cases} 0 & z < 0 \\ \delta \sin^2 \dfrac{\pi z}{2a} & 0 < z < a \\ \delta & z > a \end{cases}$$

where z is an axial co-ordinate measured from the crack tip, θ is the azimuthal angle, a is the length of the crack tip region within which the tube wall deformation occurs and δ is the maximum radial displacement. Assuming no circumferential straining, the crack opening is equal to $2\pi w(z, \pi)$.

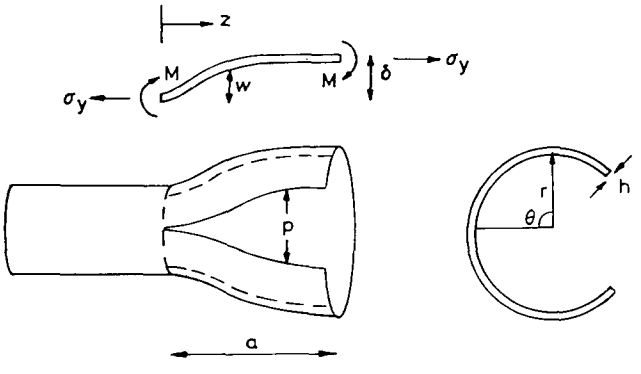

Fig. 1. Geometry of an axially propagating crack in a ruptured tube, with the paths of possible multiple cracks shown as dotted lines.

The dimensions of the deformation, a and δ, are determined by a consideration of the equilibrium conditions of a steady state running crack. An axial element of the deforming region is shown in Fig. 1. An ideal rigid-perfectly plastic material is considered. The element is acted upon by the internal pressure, axial stresses in the tube wall, and a cohesive stress acting at the crack tip. In addition, bending moments are introduced due to the curvature at the ends. The precise determination of the system of forces and moments is difficult however. To begin with, the exact distribution of internal pressure along the element is not known, though models have suggested an exponentially decaying pressure profile when the tube is gas pressured. Secondly, the element is subjected to a combination of tension and bending, the precise mixture determined by the location of the undeformed neutral axis along the element. Thirdly, azimuthal plastic bending complicates the stress analysis in the axial elements, with the consequence that axial stresses below the yield stress are sufficient for plastic yield. With all these complications present, the approach used here has been to use maximum stresses and moments, and to investigate the resulting form of the mechanics equations. The terms will be altered in a more careful treatment only by numerical coefficients.

Accordingly, the axial tensile stress on the element is taken to be σ_y and the bending moment on each end is $\sigma_y h^2/4$, where σ_y is the yield stress and h the wall thickness. The internal pressure is assumed to be a constant p throughout the deforming region. This is illustrated in Fig. 1. Equilibrium of moments about the crack tip then gives

$$\tfrac{1}{2} p a^2 = 2\sigma_y h^2/4 + \delta h \sigma_y \qquad (1)$$

which provides a link between the two unknown geometrical parameters, a and δ. The complete determination of the geometry requires another relationship specifying a or δ and this will be discussed in the next section.

As in the previous study,[2] knowledge of the crack geometry allows a calculation of the

various energy flows to proceed. In a steady state, the energy sources, namely work done on the tube by the internal pressure, plus elastic relaxation following fracture, should balance the energy dissipation, comprising fracture work, plastic work and kinetic losses. The work rate performed by the internal pressure is

$$\dot{W} = \int_{-\pi}^{\pi} \int_{0}^{a} r \, dz \, d\theta p \dot{w} \tag{2}$$

where r is the radius of the tube. Rates of change of energies are consistently replaced in the following by calculations of work done divided by a timescale a/v, where v is the crack velocity. Accordingly

$$\dot{W} = \pi r \, \delta v p \tag{3}$$

Similarly, the elastic energy release rate $\dot{\Lambda}$ is

$$\dot{\Lambda} = \pi r h v \sigma_\theta^2 / E \tag{4}$$

where σ_θ is the hoop stress ahead of the crack (equal to pr/h) and E is Young's modulus.

The dissipative mechanism of fracture surface creation leads to a work rate

$$\dot{F} = K^2 h v / E \tag{5}$$

where K is the fracture toughness. The rate of plastic work can be considered as the sum of two components corresponding to bending in the azimuthal and axial directions. Azimuthal bending leads to a work rate

$$\dot{\Gamma}_{az} = \frac{\pi}{4} \delta v \sigma_y \frac{h^2}{r} \tag{6}$$

For axial bending, taking account of the subsequent unbending of the deformed section, the dissipation rate is

$$\dot{\Gamma}_{ax} = \pi^2 \, \delta v \sigma_y r h^2 / a^2 \tag{7}$$

Both calculations assume a rigid-perfectly plastic material and take no account of the biaxial stress conditions. The ratio of $\dot{\Gamma}_{ax}$ to $\dot{\Gamma}_{az}$ is $\pi(2r/a)^2$. Therefore plastic work is dominated by axial bending for short cracks (compared to the radius) while azimuthal bending is more important for long cracks. At this point the treatment of pipe rupture propagation by Freund & Parks[4] should be mentioned. There, it was explicitly assumed that the deforming region was four times the radius of the pipe, and so $\dot{\Gamma}_{ax}$ was ignored.

Finally, the kinetic energy dissipation rate can be calculated, corresponding to the need to bring the tube wall into motion. This is

$$\dot{T} = \frac{\pi^3}{8} \rho_c h r \, \delta^2 v^3 / a^2 \tag{8}$$

where ρ_c is the density of the tube material.

The various rates, eqns (3)–(8), differ only by numerical coefficients from the corresponding terms calculated previously.[2] This is due to the revised azimuthal geometry.

In steady state:

$$\dot{T} + \dot{\Gamma}_{ax} + \dot{\Gamma}_{az} + \dot{F} = \dot{W} + \dot{\Lambda} \tag{9}$$

which leads to an equation for the crack velocity,

$$v^2 = \frac{8a^2}{\rho_c \, \delta h \pi^2} \left(p - \frac{\pi \sigma_y h^2}{a^2} - \frac{\sigma_y h^2}{4r^2} + \left(\sigma_\theta^2 - \frac{K^2}{\pi r} \right) \frac{h}{E\delta} \right) \tag{10}$$

if the right-hand side of this equation is positive, and $v = 0$ otherwise. Equation (1) determines one of a or δ in terms of the other, leaving just one unknown parameter.

The maximum bending strains in the tube wall are

$$\varepsilon_z = \frac{\delta h \pi^2}{4a^2} \tag{11}$$

for axial bending and

$$\varepsilon_\theta = \frac{\delta h}{2r^2} \tag{12}$$

for azimuthal bending. Previously, setting ε_z to the remaining ductility of the tube material supplied a relation between a and δ but the above analysis now allows this unrealistic assumption to be avoided. Comparing ε_z with the ductility now provides the desired criterion for fragmentation. This would be initiated by circumferential cracking from the tip of the axial crack, followed by the appearance of additional axial cracks, as illustrated in Fig. 1.

3 GAS PIPELINE RUPTURE

To test the model described in Section 2 we use experimental data on the propagation of axial cracks in large diameter gas pipelines.[4–8] These studies were designed to improve safeguards against the propagation of a crack for large distances away from a gas pipeline failure site. The main differences between the gas pipe and the fuel pin cases are that (a) the dimensions are

very different and (b) the pressurising medium for the gas pipe studies was air or natural gas whereas for the fuel pin the internal pressure can be provided by solid or molten fuel, or possibly by fission gas alone. Behaviour can be greatly affected by the nature of the pressurising medium, since it determines the loading profile.[9]

For the gas pipeline case, a model of gas decompression is needed in order to relate the crack driving pressure p to the initial pressure in the pipe, p_L. A one-dimensional gas dynamics treatment provides the pressure which is maintained at the tip of a crack running at velocity v.[8,10] If the crack velocity is greater than the speed of sound in the gas v_s, then $p = p_L$, otherwise

$$p = p_L\left(\frac{2}{\gamma+1} + \frac{\gamma-1}{\gamma+1}\frac{v}{v_s}\right)^{2\gamma/(\gamma-1)} \qquad (13)$$

where γ is the ratio of specific heat of the gas at constant pressure to that at constant volume. This result is derived from a model where gas is allowed to escape from a semi-infinite duct, the end of which moves at a velocity v. With $\gamma \approx 1{\cdot}4$ for air, eqn (13) implies a minimum driving pressure of $0{\cdot}28p_L$.

This model for gas decompression must be coupled to the crack velocity expression, eqn (10), in order to produce a self-consistent steady state. This procedure is illustrated in Fig. 2, which represents conditions used in test A31(CA4) of the programme carried out by Maxey *et al.*[6] for the American Gas Association. The pipe was pressurised with natural gas with $\gamma = 1{\cdot}3$ and $v_s = 396\ \mathrm{ms}^{-1}$. The v–p decompression curve is illustrated, with p_L equal to 7·92 MPa, the initial pressure in the test. The yield stress was 484 MPa, $r = 46$ cm and $h = 0{\cdot}84$ cm, so p_L was about 90% of the yield pressure $p_y = \sigma_y h/r$, which was 8·84 MPa.[4] Assigning a value of fracture toughness is rather uncertain, unfortunately. Standard pipeline steel (X60 grade) is asserted to have a toughness of 439 MPa $\mathrm{m}^{1/2}$.[15] A procedure based on equating

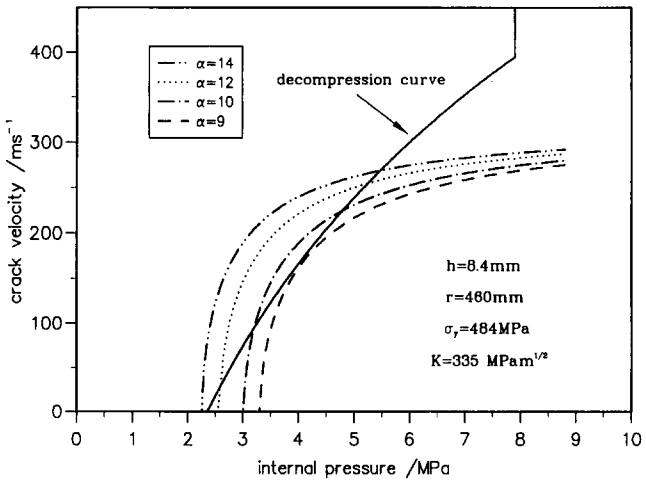

Fig. 2. Crack velocities against internal pressure in gas pipeline test A31(CA4). Also shown is the decompression pressure expected from gas dynamics.

measured Charpy energies with K^2/E leads to a value of 335 MPa $\mathrm{m}^{1/2}$.[4] Fortunately, calculations seem not to depend strongly on the precise value (see Table 1) and the latter has been used. A set of velocity curves are shown in Fig. 2, derived from eqn (10), over the full range of crack driving pressures from 0 to p_y. The remaining geometrical uncertainty in the model, referred to earlier, is removed by the parametrisation

$$a^2 = \alpha r h \qquad (14)$$

where α is a constant. This form has been used in some other treatments[6] with $\alpha = 9$, based upon the observed transition from propagating to arrested cracks as a function of pressure. Young's modulus was taken to be 2×10^5 MPa and the steel density was 7770 kg m^{-3}.

Self-consistent steady propagation conditions occur where the crack velocity and decompression curves intersect. An additional requirement is that the decompression curve should have the greater slope at the intersection. This ensures the situation is stable: if the crack ran faster, the driving pressure would increase, but would take the tube into the net energy dissipating region above the steady crack velocity curve shown.

Table 1. Analysis of US tests of crack propagation in gas pipelines

Test	r (mm)	h (mm)	p_L (MPa)	σ_y (MPa)	K (MPa $\mathrm{m}^{1/2}$)	v (ms^{-1}) (model)	v (ms^{-1}) (expt)	Comments
A31(CA4)	460	8·4	7·92	484	335	261	216–307	Natural gas[4,6]
					439	253		
A32(CA5)	460	8·4	5·86	459	335	225	221–253	Natural gas[6,8]
SF-12W	530	9·5	6·41	531	335	269	244	Air test[4,5]

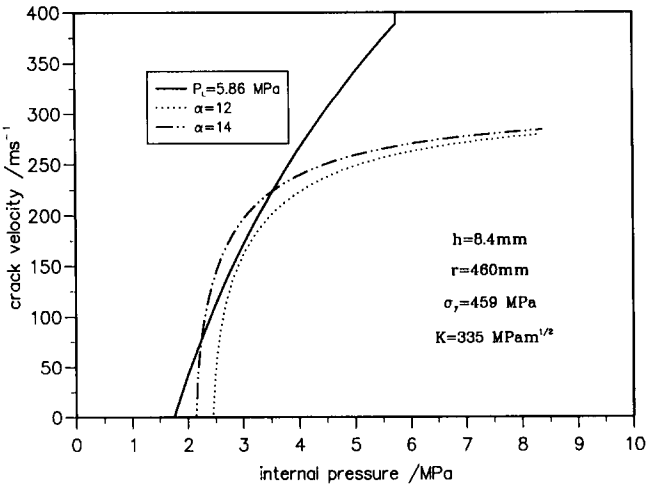

Fig. 3. Crack velocity against internal pressure for gas pipeline test A32(CA5). Also shown is the appropriate decompression curve.

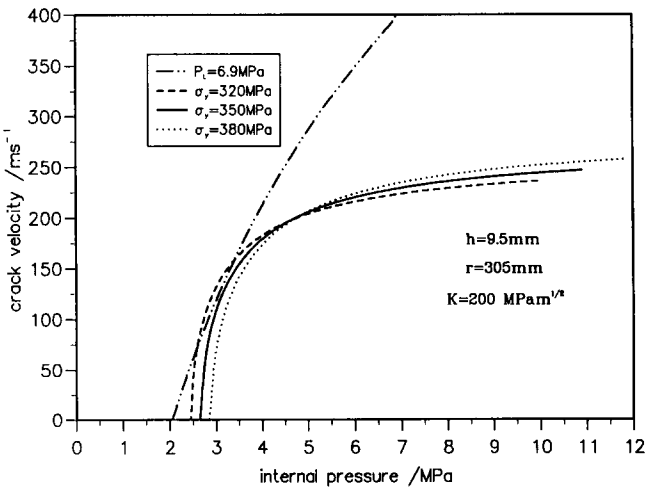

Fig. 5. Crack velocity against pressure for British Gas pipeline test 9. Curves for a range of material yield stress are shown.

This would return the system to equilibrium. The intersection at the higher pressure is therefore selected; the low pressure intersection being unstable.

Since the experimental velocity was reported to be 260 ms^{-1} (with an uncertainty of about 20%), this constrains α to be in the range 12–14. This is checked in Fig. 3 which shows calculations made for test A32(CA5).[6,8] The crack velocity for this test was reported to lie in the range 221–253 ms^{-1}. From these analyses, $\alpha = 14$ is selected as the best fit. Results are equally encouraging for tests SF-12W[5] which used air as the pressurising medium, with $\gamma = 1{\cdot}4$ and $v_s = 341$ ms^{-1}. Figure 4 demonstrates that the intersection of the crack velocity curve and the decompression curve starting from an initial, experimental, pressure of 6·41 MPa, lies not far away from the observed crack speed of 244 ms^{-1}. Also shown are decompression curves starting from 5 MPa and the yield pressure p_y of 9·52 MPa. Possible crack velocities clearly lie between about 300 ms^{-1} and about 200 ms^{-1}, depending on p_L. Below a critical initial pressure, the crack will not propagate in a stable fashion. Equivalently, there is a minimum crack driving pressure, in this case about 3·2 MPa, or $0{\cdot}37 p_y$. This corresponds quite well to the arrest/propagate transition stress proposed by Maxey *et al.*, which is approximately $0{\cdot}3p_y$.[6,11] The analysis of the US tests is summarised in Table 1.

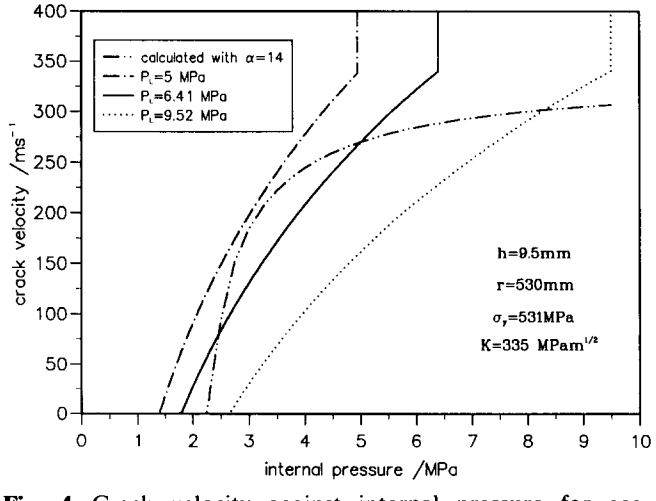

Fig. 4. Crack velocity against internal pressure for gas pipeline test SF-12W. Several gas decompression curves are shown for a range of initial pressures.

A further example is shown in Fig. 5. This is meant to represent a test in a British Gas study.[7] The pressurising medium was natural gas. Unfortunately, experimental conditions were not reported clearly in Ref. 7, corresponding to an uncertainty in the tube material yield stress. Furthermore, it is suggested that the pipe steel fracture toughness is less than in the US tests, though nominally a similar material (grades X52 and X60). A value of 200 MPa m$^{1/2}$ has been used, based on reported Charpy energies.[7] Correspondingly, the yield stresses examined are lower than in the US tests. Crack velocities between 36 ms^{-1} and 125 ms^{-1} were observed for this geometry, the fastest crack propagation being consistent with the intersections shown in the figure, where velocity curves are drawn for a number of yield stresses. Considering the uncertainties in a number of the required

parameters, the British Gas study provides only qualitative support for the proposed model.

It is useful at this stage to compare the present model with that of Freund and Parks,[4] who made a similar analysis of energy sources and sinks. The main geometrical difference compared to the present treatment is the inclusion of an unfractured membrane of material a distance R into the deforming crack tip region. The crack opening is given by the critical displacement.[14] The geometry is determined by the choices $a = 4r$ and $R = 0{\cdot}75r$, axial bending is ignored and the driving pressure is assumed to decay linearly between $z = 0$ and $z = a$. The resulting crack velocity curve for test A31(CA4) is shown in Fig. 6 (compare with Fig. 2). The decompression curve and crack velocity curve intersect at about the right velocity, but the equilibrium is unstable and would not be supported for long.

The axial bending strain for all of the gas pipeline tests is about 0·5–1% for stable propagation conditions. This is well below the ductilities expected of pipeline materials and so the model is consistent with the observed absence of multiple cracking. The azimuthal bending strains are smaller. Typical radial displacements lie in the range 1·5–3 cm for these tests, corresponding to crack openings of about 9–18 cm or about 0·4 radii. Often much larger displacements have been seen which may indicate a deficiency in the modelling. However, the success in accounting for propagation conditions is encouraging enough to apply the model to fuel pin ruptures.

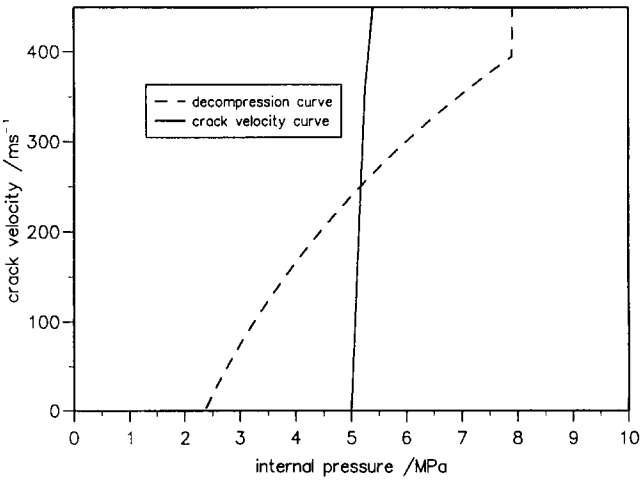

Fig. 6. Crack velocity predictions from Ref. 4 together with decompression curve for test A31(CA4), for comparison with Fig. 2.

4 FUEL PIN RIP PROPAGATION

The missing element of a complete model of crack propagation in ruptured fuel pins is a description of pin depressurisation. Unless the fuel–clad gap is open at failure, in which case the pin is effectively gas pressurised, the previous model cannot be used. Preliminary calculations of relaxation of a compressed solid bar, on releasing the load at one end, do not yield an equivalent description of a finite crack tip pressure as in eqn (13), but rather predict a step-like decompression front moving away from the fracture at the speed of sound in the bar. In the absence of an adequate model, however, predictions can still be made. Figure 7 shows the results of crack velocity calculations, with $\alpha = 14$, for a tube typical of fuel pin cladding with $r = 4$ mm, $h = 0{\cdot}5$ mm, $\sigma_y = 300$ MPa and $K = 100$ MPa m$^{1/2}$. The yield pressure was 37·5 MPa. Over the range of possible driving pressures, the crack velocity ranges from 0 to about 225 ms^{-1}, with a minimum driving pressure of about 12 MPa or $0{\cdot}32p_y$. The actual driving pressure will depend on the initial pressure and the decompression mechanism. If the pressurising medium was a high-temperature gas, with a higher speed of sound than in the case of the low-temperature gas pipe tests, then the decompression curve would intersect with the crack velocity curve in the 12–15 MPa driving pressure range, with $v \approx 100$ ms^{-1}.

Figure 7 also shows the axial bending strain, ε_z, over the possible range of pressure. Where v is non-zero, ε_z ranges between about 4% and 14%. For the gas depressurisation case, ε_z would lie between 4% and 7%. Whether the tube fragments then depends on the available ductility of the material. This is affected by the temperature, strain rate and irradiation history, and predictions therefore depend on the precise conditions at failure. For many years 20% CW AISI 316 stainless steel has been a benchmark fast reactor fuel pin cladding material, and its properties are well established. Figure 8 reproduces CABRI-1 data reported in Ref. 12 on the uniform elongation (UE) of this material, at a high strain rate of 5 s^{-1} and over a range of temperatures. A reduction in UE is apparent after irradiation. Pins with the dimensions and properties given above and fractured, for

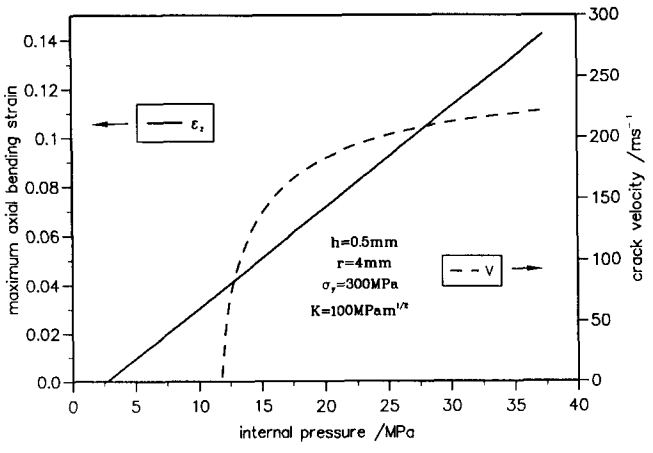

Fig. 7. Axial bending strain and crack velocity against internal pressure, for fuel pin geometry.

example, at 1000°C would therefore be likely to fail with a single crack geometry before irradiation, but fragment after irradiation. The crack length at the onset of fragmentation would be about $2a$ or $2(14rh)^{1/2}$ which is about 10·6 mm for the given geometry, just over one diameter of the pin.

The revised crack propagation model has been included within the TRAFIC fuel pin modelling code[13] and used in the analysis of a selection of failure tests in the CABRI-1 programme.[1] These involve subjecting a fuel pin to an overpower transient, such that the cladding tube experiences high stresses. The pin cladding material was 20% CW AISI 316. The results are shown in Table 2. A range of ε_z can be deduced corresponding to possible crack velocities between zero and the

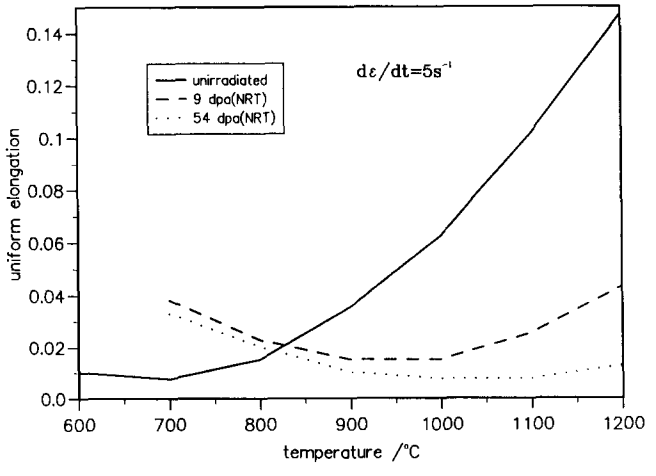

Fig. 8. Dependence of uniform elongation of 20% CW AISI 316 steel on test temperature and irradiation history.

Table 2. Calculations of axial bending strains, ε_z, and upper limits on crack velocities, v, for tests in the CABRI-1 series,[1] assuming $\sigma_\theta = \sigma_y$

Test	A3	BI2	AI3	BI4
σ_θ (MPa)	278	255	543	275
T (°C)	720	896	685	1129
ε_z	4–15%	3·5–14%	3·4–16%	3·5–15%
v (ms^{-1})	212	205	300	212

maximum velocity shown. The temperature of the test allows comparison of ε_z with the clad ductility: test A3 used a fresh pin and the others involved pins irradiated to 9 dpa(NRT). The CABRI-1 programme included many other tests, some on pins irradiated to 60 dpa(NRT), but this sample set will serve as an illustration of the model. In all cases, the minimum axial bending strain exceeds the uniform elongation and so multiple cracking would seem to be favoured. It is not easy to distinguish between single and multiple cracking however, due to the destruction of the pin later in the transient, but measurements do indicate an initial axial extent of the pin rupture of about 2 cm,[1] similar to the estimated length suggested above at which arrest by fragmentation occurs.

5 DISCUSSION

The model of axial crack propagation in ruptured tubes developed here is based on the mechanics of crack geometry and energy flows. Using a model of gas decompression at the tip of a running crack, a description of the propagation of a rupture in 1 m-diameter gas pipes has been developed which has a number of desirable features. Firstly, it can account for the propagation velocities of cracks in a number of gas pipeline tests. Secondly, a minimum initial pressure for steady propagation emerges, consistent with the threshold suggested by Maxey *et al.*[6,11] Thirdly, the propagation conditions are stable with respect to small perturbations. In this respect the model is more satisfactory than that developed by Freund and Parks.[4] The model has been applied to the interpretation of fuel pin rupture tests in the CABRI-1 programme.[1]

The model developed here from earlier work[2] contains a criterion for the appearance of multiple cracks. This is encountered when axial

bending strains greater than the ductility are produced in the flaps behind the crack tip. Strains are low (about 1%) for the gas pipeline tests, but relatively high (up to 15%) in calculations of fuel pin rupture. This reflects a proportionality between ε_z and h/r, which leads from eqns (1), (11) and (14). Multiple cracking therefore appears likely in fuel pin cases, especially after irradiation when ductilities are low (Fig. 7 and Ref. 12). This would limit the axial extension of a pin rupture but increase the area of fracture compared with the single crack mode.

Further work would be necessary in order to refine the model and examine the sensitivity of the fragmentation criterion to uncertainties in the mechanics discussed earlier. The form taken by the deformation is assumed and parametrised by radial displacement δ and axial extent a. A functional relation between the two is found by an approximate mechanical analysis, and the other is fitted to data. The tube is treated as a thin shell, and the wall material is taken to be rigid–perfectly plastic. Future development ought to improve the mechanical analysis, taking into account stress biaxiality and combined bending and tension, as well as a realistic axial profile of driving pressure. Some allowance for elastic bending and work hardening should be made. For fuel pins, the decompression of molten fuel should be considered in greater depth than hitherto.[2] Data on the rupture of gas pressurised fuel pins would be extremely useful. Nevertheless, the model seems to describe the data quite well and probably contains the essence of the physics involved.

6 CONCLUSIONS

The results of this study can be summarised as follows:

(a) An analysis of energy flows in a propagating crack, together with a model of gas depressurisation can account for observed crack velocities in gas pipes, and the stability of propagation.
(b) A criterion for tube wall multiple cracking and fragmentation has been suggested, based on a comparison of material ductility and likely bending strains.
(c) The model has been applied to the case of the rupture of fast reactor fuel pins.
(d) Fuel pin failure driven by gas or molten fuel is likely to result in cladding fragmentation and a limited axial extent of rupture, due to the large ratio of wall thickness to tube radius, and the low material ductility. Gas pipe rupture is unlikely to result in fragmentation.
(e) Experimental confirmation of the fragmentation criterion is lacking at present.

ACKNOWLEDGEMENT

This work was performed as part of the Fast Reactor Safety Programme of AEA Technology, on behalf of the UK Department of Trade and Industry.

REFERENCES

1. Cranga, M., Struwe, D., Pfrang, W., Brear, D. J. & Nonaka, N., Transient material behaviour in CABRI-1 experiment failure under fully and semi-restrained fuel pin conditions. *Proceedings of the 1990 International Fast Reactor Safety Meeting*, Snowbird, Utah. American Nuclear Society, Vol. 1, p. 421.
2. Ford, I. J., Axial crack propagation in fuel pin cladding tubes. Harwell Report AEA-InTec-0620, August 1991. *J. Nucl. Eng.* and *Design*, **136** (1992) 243.
3. Buxton, K., Pemberton, G. W. & Linekar, G. A. B. (unpublished).
4. Freund, L. B. & Parks, D. M., Analytical interpretation of running ductile fracture experiments in gas-pressurised linepipe. *Crack Arrest Methodology and Applications, ASTM STP 711*, ed. G. T. Hahn & M. F. Kanninen. 1980, p. 359.
5. Ives, K. D., Shoemaker, A. K. & McCartney, R. F., *J. Eng. Materials and Technology*, **96** (1974) 309.
6. Maxey, W. A., Kiefner, J. F., Eiber, R. J. & Duffy, A. R., In *Proc. 12th World Gas Conference*. International Gas Union, Nice, France, 1973.
7. Fearnehough, G. D., *Int. J. Pres. Ves. and Piping*, **2** (1974) 257.
8. Kanninen, M. F., Sampath, S. G. & Popelar, C., *J. Pressure Vessel Technology*, **98** (1976) 56.
9. Ford, I. J., Axial cracking of cladding tubes loaded by solid fuel pellets. Harwell Report AEA-InTec-0782, January 1992.
10. Liepmann, H. W. & Roshko, A., *Elements of Gasdynamics*. Wiley, New York, 1957, p. 62.
11. Maxey, W. A., Podlasek, R. J., Eiber, R. J. & Duffy, A. R., Observations on shear fracture behaviour. British Gas/IGE Symposium: Crack Propagation in Pipelines, Newcastle, March 1974.
12. Balourdet, M. & Cauvin, R., Transient mechanical properties of CABRI-1 cladding (CW 316). *Proc. BNES Conf. on Fast Reactor Core and Fuel Structural*

Behaviour, Inverness, 1990. British Nuclear Energy Society, London.
13. Matthews, J. R., Cameron, R. F., Coleman, P. E. & Thetford, R., The application of the TRAFIC code to fast reactor fuel transients. *Proc. BNES Conference on Fast Reactor Safety*, Guernsey, UK, May 1986. British Nuclear Energy Society, London.
14. Brock, D., *Elementary Engineering Fracture Mechanics*. Sijthoff and Noordhoff, Alphen aan den Rijn, The Netherlands, 1978, Chap. 9.
15. Hahn, G. T., Sarrate, M., Kanninen, M. F. & Rosenfield, A. R., *Int. J. Fracture*, **9** (1973) 209.